

Friedel Oscillations, Impurity Scattering, and Temperature Dependence of Resistivity in Graphene

Vadim V. Cheianov and Vladimir I. Fal'ko

Physics Department, Lancaster University, Lancaster, LA1 4YB, United Kingdom

(Received 10 August 2006; published 28 November 2006)

We show that Friedel oscillations (FO) in graphene are strongly affected by the chirality of electrons in this material. In particular, the FO of the charge density around an impurity show a faster ($\delta\rho \sim r^{-3}$) decay than in conventional 2D electron systems and do not contribute to a linear temperature-dependent correction to the resistivity. In contrast, the FO of the exchange field which surrounds atomically sharp defects breaking the hexagonal symmetry of the honeycomb lattice lead to a negative linear T dependence of the resistivity.

DOI: [10.1103/PhysRevLett.97.226801](https://doi.org/10.1103/PhysRevLett.97.226801)

PACS numbers: 73.43.Cd, 73.63.Bd, 71.70.Di, 81.05.Uw

Screening strongly influences properties of impurities in metals and semiconductors. While Thomas-Fermi screening suppresses the long-range tail of a charged impurity potential, Friedel oscillations (FO) of the electron density around a defect [1] are felt by scattered electrons at a distance much longer than the Thomas-Fermi screening length. Friedel oscillations originate from the singular behavior of the response function of the Fermi liquid at wave vector $2k_F$. At zero temperature, the decay of the amplitude $\delta\rho$ of these oscillations with distance r from the impurity obeys a power law dependence. In a nonrelativistic degenerate two-dimensional (2D) Fermi gas [2], $\delta\rho \propto \cos(2k_F r + \delta)/r^2$. In 2D electron systems, Bragg scattering off the potential created by these long-range FO strongly renormalizes the momentum relaxation rate τ^{-1} for quasiparticles near the Fermi level $\epsilon \approx \epsilon_F$, which leads to a linear temperature dependence of the resistivity [3–6] in a “ballistic” temperature range $\epsilon_F > T > h/\tau$ confirmed in recent experiments on semiconductor heterostructures and Si field-effect transistors [7].

The graphene-based transistor [8,9] is a recent invention which attracts a lot of attention. Improvement of the performance of this device requires identification of the dominant source of electron scattering limiting its mobility. Those can be structural defects of graphene lattice (vacancies and dislocations), substitutional disorder, chemical deposits on graphene, and, importantly, charges trapped in or on the surface of the underlying substrate.

In this Letter, we investigate the effects of screening of scatterers in graphene and show how the phenomenon of FO can be used to gain insight into the microscopic nature of disorder. Graphene (a monolayer of graphite) is a gapless 2D semiconductor with a Dirac-like dispersion of carriers [10]. In this material, it is the Thomas-Fermi screening which is responsible [11] for the experimentally observed linear dependence of graphene conductivity on the carrier density [8,9]. Moreover, quasiparticles in graphene possess chiral properties related to the sublattice composition of the electron wave on a 2D honeycomb lattice [10]. Below, we show that, due to the latter peculiarity of graphene, FO of the electron density decay as

$\delta\rho \sim r^{-3}$ at a long distance from an impurity [faster than in a usual 2D metal], and the linear temperature-dependent correction to the resistivity

$$R(T) - R(0) = -\frac{h}{e^2} \frac{T\hbar}{\epsilon_F^2 \tau_*} \quad (1)$$

is caused only by the FO of the exchange field and is strongly sensitive to the microscopic origin of scatterers. In Eq. (1), τ_*^{-1} is the backscattering rate specifically from atomically sharp defects distorting the hexagonal symmetry of the honeycomb lattice: structural defects, chemical deposits, and substitutional disorder. Note that Coulomb scatterers do not contribute towards this result. Thus, we predict that, in graphene-based devices where scattering is dominated by charges trapped in the substrate (or on its surface), the temperature-dependent resistivity $[R(T) - R(0)]/R \sim (T/\epsilon_F)(\tau/\tau_*)$ is much weaker than in conventional 2D semiconductor structures. We propose to use the measurement of the resistivity in a temperature range $\epsilon_F > T > h/\tau$ as a probe of the composition of disorder.

Electrons in graphene can be described using 4-component Bloch functions $[\phi_{\mathbf{K}_+,A}, \phi_{\mathbf{K}_+,B}, \phi_{\mathbf{K}_-,B}, \phi_{\mathbf{K}_-,A}]$, which characterize the electronic amplitudes on the two sublattices (A and B) and valleys \mathbf{K}_+ and \mathbf{K}_- . Since for the ballistic temperature regime $T\tau/h > 1$ interference between waves scattered from FO around different impurities can be neglected, we study screening of an individual impurity. The single-particle Hamiltonian in the presence of one impurity is

$$\hat{H}_{\text{sp}} = -i\hbar v \boldsymbol{\Sigma} \cdot \nabla + \hat{u} \delta(\mathbf{r}). \quad (2)$$

In this expression, $\boldsymbol{\Sigma} = (\boldsymbol{\Sigma}_x, \boldsymbol{\Sigma}_y)$ is a two-dimensional vector whose components are 4×4 matrices $\boldsymbol{\Sigma}_x = \Pi_z \otimes \sigma_x$ and $\boldsymbol{\Sigma}_y = \Pi_z \otimes \sigma_y$. Together with $\boldsymbol{\Sigma}_z = \Pi_0 \otimes \sigma_z$, they form [12] the generator algebra of the unitary group SU_2^Σ . Here $\Pi_{x,y,z}$ and $\sigma_{x,y,z}$ are sets of three Pauli matrices acting on the valley and sublattice indices, respectively, and Π_0 (σ_0) are 2×2 unit matrices acting on the valley (sublattice) spaces. Another set of three matrices, $\Lambda_x = \Pi_x \otimes \sigma_z$, $\Lambda_y = \Pi_y \otimes \sigma_z$, and $\Lambda_z = \Pi_z \otimes \sigma_0$, such that

$[\Lambda_{l_1}, \Lambda_{l_2}] = 2i\epsilon^{l_1 l_2 l} \Lambda_l$, satisfies $[\Sigma_s, \Lambda_l] = 0$. Therefore, they commute with the first term in \hat{H}_{sp} and generate the unitary group $SU_2^\Lambda \equiv \{e^{i\mathbf{b}\hat{\Lambda}}\}$ describing the valley symmetry of the Dirac Hamiltonian in graphene.

For a nonmagnetic defect, the matrix \hat{u} in Eq. (2) should be Hermitian and time-reversal symmetric. It can be parametrized using 10 independent real parameters [12,13]. One can check [12,14] that all of the operators Σ_s and Λ_l change sign under the time-reversal transformation, so that the 9 products $\Sigma_s \Lambda_l$ are $t \rightarrow -t$ invariant and together with the unit matrix $\hat{I} = \Pi_0 \otimes \sigma_0$ can be used as a basis to represent a nonmagnetic static disorder:

$$\hat{u} = u\hat{I} + \sum_{s,l=x,y,z} u_{sl} \Sigma_s \Lambda_l \equiv u\hat{I} + X_z \Sigma_z + \mathbf{X} \cdot \boldsymbol{\Sigma},$$

$$X_s = \sum_{l=x,y,z} u_{sl} \Lambda_l. \quad (3)$$

The term $u\hat{I}$ in Eq. (3) represents an electrostatic potential averaged over the unit cell. We attribute this term to charged impurities with a sheet density n_c . Various atomically sharp defects [15] with the 2D density n_{def} can be parametrized using nine independent real parameters u_{sl} and time-inversion-symmetric [14] matrices $\Sigma_s \Lambda_l$. In particular, u_{zz} describes different on-site energies on the *A* and *B* sublattices. Terms with u_{xz} and u_{yz} take into account fluctuations of $A \leftrightarrow B$ hopping, whereas u_{sx} and u_{sy} ($s = x, y, z$) generate intervalley scattering (whose presence has been revealed [12] by the observation of weak localization in graphene [16]).

The momentum relaxation of chiral electrons in graphene due to scattering off Coulomb impurities is determined by the anisotropic differential cross section

$$w(\theta) \sim u_{k_F}^2 \sin(\theta/2) \cos^2(\theta/2).$$

The factor $\cos^2(\theta/2)$, where θ is the scattering angle, reflects the absence of backscattering of graphene electrons off the electrostatic potential [17,18]. In the RPA, the Fourier transform u_q of the electrostatic potential of a single charged impurity screened by 2D electrons is $u_q = 2\pi(e^2/\chi)/(q + \kappa)$, where $\kappa = 8\pi\gamma e^2/\chi = 4k_F r_s$; $\gamma = k_F/(2\pi\hbar v)$ is the density of states per spin and valley, χ is the dielectric constant, and $r_s \equiv e^2/\chi\hbar v$ (for a graphene sheet on a Si substrate, $r_s \sim 1$).

In a structure with sheet density n_c of charged impurities, the resistivity $R = [2e^2\gamma v^2\tau]^{-1}$ is determined by the momentum relaxation rate $\tau^{-1} \sim n_c\pi\gamma\hbar^{-1}\langle(1 - \cos\theta)w(\theta)\rangle_\theta$, and it is inverse proportional to the carrier density n_e [11]:

$$R = \frac{h}{4e^2} \frac{n_c}{n_e} \frac{4\pi\eta(r_s)r_s^2}{(1 + 4r_s)^2}, \quad (4)$$

where $\eta(r_s)$ is a monotonous function such that $\eta(0) = 1$, $\eta(1) \approx 0.3$, and $\eta(\infty) = \frac{1}{4}$. It has been established that a contribution from atomically sharp disorder towards R

depends on the Fermi energy only logarithmically [13]. Therefore, the empirical relation $n_e R = \text{const}$ established in the experimentally studied graphene structures with high carrier densities [8,9] indicates that charges located in the underlying substrate or on its surfaces are the main source of scattering. In Eq. (3), it is represented by $u\hat{I}$.

Analysis of Friedel oscillations.—Below, we analyze the FO of the density matrix of 2D electrons in graphene surrounding various types of scatterers, Eq. (3). The plane wave eigenstates of the Dirac Hamiltonian $-i\hbar v \boldsymbol{\Sigma} \cdot \nabla$ are $\psi_{\mathbf{k},\xi}(\mathbf{r}) = e^{i\mathbf{k}\mathbf{r}}|\mathbf{k}\xi\rangle$. Here the spinor $|\mathbf{k}\xi\rangle$ has a definite valley projection, $\Lambda_z|\mathbf{k}\xi\rangle = \xi|\mathbf{k}\xi\rangle$, $\xi = \pm 1$, and chirality: the projection $\boldsymbol{\Sigma} \cdot \mathbf{n} = \pm 1$ of the operator $\boldsymbol{\Sigma}$ on the direction of motion $\mathbf{n} = \mathbf{k}/k$. Below, we describe a chiral electron with $\boldsymbol{\Sigma} \cdot \mathbf{n} = 1$ using the polarization matrix

$$\hat{s}_{\mathbf{n}} \equiv \sum_{\xi=\pm 1} |\mathbf{k}\xi\rangle\langle\mathbf{k}\xi| = \frac{1}{2}(\mathbf{1} + \boldsymbol{\Sigma} \cdot \mathbf{n}), \quad \hat{s}_{\mathbf{n}}^2 = \hat{s}_{\mathbf{n}}. \quad (5)$$

Because of scattering off the impurity, the plane wave eigenstates of the Hamiltonian acquire a correction $\delta\psi_{\mathbf{k},\xi}$, which in the Born approximation is given by

$$\delta\psi_{\mathbf{k},\xi}(\mathbf{r}) = \int \frac{d^2p}{(2\pi)^2} \frac{e^{i\mathbf{p}\mathbf{r}}}{E(k) - \hbar v \boldsymbol{\Sigma} \cdot \mathbf{p} + i0} \hat{u}|\mathbf{k}\xi\rangle. \quad (6)$$

Here $E(k) = \pm\hbar vk$, where the sign $+$ ($-$) corresponds to the conduction (valence) band states. For graphene with the Fermi energy ϵ_F positioned in the conduction band, and for $T < \epsilon_F$, we shall disregard the valence band contribution. Then the correction to the electron density matrix induced by the impurity is

$$\delta\hat{\rho}(\mathbf{r}, \mathbf{r}') = \int \frac{d^2k}{(2\pi)^2} n_F(k) \delta\psi_{\mathbf{k},\xi}(\mathbf{r}) \otimes \psi_{\mathbf{k},\xi}^\dagger(\mathbf{r}') + \text{H.c.} \quad (7)$$

The matrix $\delta\hat{\rho}(\mathbf{r}, \mathbf{r}')$ contains a slowly decaying oscillatory part, which is due to a jump in the Fermi function $n_F(k)$. After substituting Eq. (6) into Eq. (7) for the density matrix, we find that, in the region $1 < k_F r < \epsilon_F/T$, the oscillating part of the “local” density matrix $\hat{\rho}(\mathbf{r}, \mathbf{r})$ calculated to leading order in $1/r$ is given by

$$\delta\hat{\rho}(\mathbf{r}, \mathbf{r}) = \frac{k_F}{8\pi 2v} \frac{e^{2ik_F r}}{2ir^2} \hat{s}_{\mathbf{n}} \hat{u} \hat{s}_{-\mathbf{n}} + \text{H.c.};$$

$$\hat{s}_{\mathbf{n}} \hat{u} \hat{s}_{-\mathbf{n}} = \frac{1}{2}(\hat{X}_z + i\mathbf{n} \times \hat{\mathbf{X}})(\hat{\Sigma}_z - i\mathbf{n} \times \hat{\Sigma}), \quad (8)$$

where $\mathbf{n} = \mathbf{r}/r$ and $\mathbf{a} \times \mathbf{b} \equiv a_x b_y - a_y b_x$. The matrix structure of $\delta\hat{\rho}$ describes the distribution of charge at the atomic length scale: oscillations with the wave vector $\mathbf{K} = \mathbf{K}_+ - \mathbf{K}_-$ (related to $\Lambda_{x,y}$) superimposed with the oscillations between the *A* and *B* sublattices (related to, e.g., Σ_z).

The FO in the density matrix (8) do not lead [19] to oscillations in the charge density $\delta n_e(\mathbf{r}) = \text{Tr} \delta\hat{\rho}(\mathbf{r}, \mathbf{r})$ because for any pair of matrices Σ_s and Λ_l , $\text{Tr} \Sigma_s \Lambda_l = 0$. To find δn_e , we evaluated $\delta\hat{\rho}$ up to order r^{-3} in the $1/(k_F r)$ expansion and arrived at the leading nonvanishing contribution to the FO of the electron density coming from the

diagonal disorder $u\hat{l}$

$$\frac{\delta n_e(\mathbf{r})}{n_e} = \frac{un_e \cos(2k_F r)}{\epsilon_F (2k_F r)^3}, \quad k_F r \gg 1, \quad (9)$$

where for a screened impurity charge $(un_e/\epsilon_F) \sim 2r_s/(1+4r_s) \sim 1$. The FO in Eq. (9) decay with the distance from the Coulomb impurity faster than in a conventional 2D electron gas (where FO obey the $1/r^2$ law). This is due to the absence of backscattering of a chiral electron off the potential $u\hat{l}$ conserving the sublattice state [17]. As a result, Bragg scattering off FO formed around the Coulomb impurity is suppressed and does not lead to a linear T dependence of the resistivity.

Interaction correction to resistivity.—Since atomically sharp defects do not generate FO in the electron density, they also do not induce an oscillating Hartree potential, though they generate a nonlocal exchange field. Below, we investigate using the Born approximation how the exchange field created by the FO in Eq. (7) renormalizes impurity scattering and leads to a linear T dependence of the resistivity. We write down the Hartree-Fock potential created by the impurity as a sum $H_H + H_F$:

$$H_H = 2 \int d\mathbf{r} d\mathbf{r}' V(\mathbf{r} - \mathbf{r}') \text{Tr} \rho(\mathbf{r}', \mathbf{r}') \psi^\dagger(\mathbf{r}) \psi(\mathbf{r}),$$

$$H_F = - \int d\mathbf{r} d\mathbf{r}' V(\mathbf{r} - \mathbf{r}') \psi^\dagger(\mathbf{r}) \rho(\mathbf{r}, \mathbf{r}') \psi(\mathbf{r}'),$$

where $V(\mathbf{r})$ is the (screened) Coulomb potential averaged over the unit cell. Here we suppressed the electron spin indices, for brevity. The factor of 2 in H_H is the result of summation over spin channels.

The leading correction $\delta w(p, \theta)$ to the differential cross section $w(\theta)$ of scattering off a defect is a result of the interference [3] between the wave scattered by the defect itself and the wave Bragg-reflected by the Hartree [Fig. 1(a)] and the Fock [Fig. 1(b)] potentials of the FO. The resulting correction to the momentum relaxation rate is

$$\delta\tau^{-1} = -n_{\text{def}} v \int dp n'_F(p) \int \frac{d\theta}{2\pi} (1 - \cos\theta) \delta w(p, \theta).$$

After substituting the Born amplitude $A(\theta)$ of the scattering process of the defect itself and the amplitudes $\delta A_{a(b)}(\theta)$ of the two processes in Figs. 1(a) and 1(b) into the differential

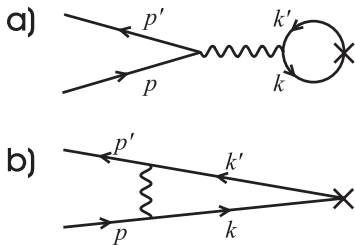


FIG. 1. The figure is a schematic representation of the processes renormalizing the scattering amplitude in (a) the Hartree and (b) the Fock channels.

cross section $w(\theta) = |A + \delta A_a + \delta A_b|^2$, one finds that $\delta w(\theta) = 2\text{Re}[A^*(\delta A_a + \delta A_b)]$, which yields

$$\delta\tau^{-1} = \frac{n_{\text{def}}}{2\pi^4 v^2} \text{Re} \int d\mathbf{p} d\mathbf{p}' d\mathbf{k} d\mathbf{k}' \delta_E \delta_M \frac{1 - \mathbf{n} \cdot \mathbf{n}'}{k^2 - (k')^2 + i0}$$

$$\times [\tilde{V}(|\mathbf{k} - \mathbf{p}|) k \Gamma_{\mathbf{p}, \mathbf{p}'}^{\mathbf{k}, \mathbf{k}'}$$

$$- 2\tilde{V}(|\mathbf{p}' - \mathbf{p}|) k \tilde{\Gamma}_{\mathbf{p}, \mathbf{p}'}^{\mathbf{k}, \mathbf{k}'}] n_F(k) n'_F(p), \quad (10)$$

where

$$k \Gamma_{\mathbf{p}, \mathbf{p}'}^{\mathbf{k}, \mathbf{k}'} = \frac{1}{2} \text{Tr}[\hat{s}_{\mathbf{n}} \hat{u} \hat{s}_{\mathbf{n}'} (k + \boldsymbol{\Sigma} \cdot \mathbf{k}') \hat{u} \hat{s}_{\mathbf{m}}],$$

$$k \tilde{\Gamma}_{\mathbf{p}, \mathbf{p}'}^{\mathbf{k}, \mathbf{k}'} = \frac{1}{2} \text{Tr}[\hat{s}_{\mathbf{n}} \hat{u} \hat{s}_{\mathbf{n}'}] \text{Tr}[(k + \boldsymbol{\Sigma} \cdot \mathbf{k}') \hat{u} \hat{s}_{\mathbf{m}}].$$

In Eq. (10), the integration is constrained by the momentum and energy conservation imposed by $\delta_M = \delta^2(\mathbf{p} - \mathbf{p}' + \mathbf{k}' - \mathbf{k})$ and $\delta_E = \delta(p - p')$, and we use the notations $\mathbf{n} = \mathbf{p}/p$, $\mathbf{n}' = \mathbf{p}'/p$, $\mathbf{m} = \mathbf{k}/k$. Two form factors of Bragg scattering Γ and $\tilde{\Gamma}$ represent the Fock and the Hartree contributions, respectively. Assuming x - y isotropy of disorder, we average the relaxation rate τ^{-1} over the directions of the initial wave vector \mathbf{p} .

The Bragg scattering correction to the momentum relaxation rate (10) can be separated into zero-temperature and temperature-dependent parts $\delta\tau^{-1} = \delta\tau_0^{-1} + \delta\tau_T^{-1}$. The linear temperature dependence of $\delta\tau_T^{-1}$ [3] is due to a singularity at $k = k'$ in the integral (10). To evaluate its contribution, we extend the analysis presented in Ref. [3]. First, we use δ_M and δ_E to rewrite the denominator in the integral (10) as $k^2 - (k')^2 = 2(\mathbf{k} - \mathbf{p})(\mathbf{p} - \mathbf{p}') = 2kp(\cos\theta - \cos\theta') - 2p^2[1 - \cos(\theta - \theta')]$, where $\theta = \angle(\mathbf{k}, \mathbf{p})$ and $\theta' = \angle(\mathbf{k}, \mathbf{p}')$. The integrand is singular at those points where the denominator vanishes, except for $\theta = \theta'$, where the singularity is cancelled by the factor $[1 - \cos(\theta - \theta')]$. For given k and p , the locus of singular points is a contour in the plane (θ, θ') , which we show in Fig. 2 for various ratios k/p . As k changes from $k < p$ to $k > p$, two parts of this contour coalesce, creating a double pole at the point $(\theta, \theta') = (0, \pi)$. We rewrite Eq. (10) as

$$\delta\tau_T^{-1} = \frac{n_{\text{def}}}{4\pi^4 v^2} \int dp dk n_F(k) n'_F(p) g(k, p) - \delta\tau_0^{-1},$$

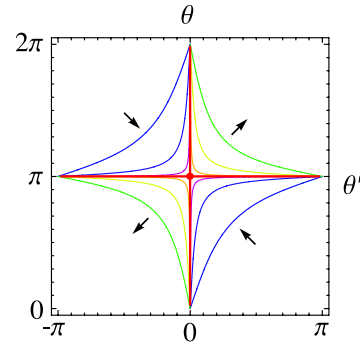


FIG. 2 (color online). The structure of singularities in the integration. The contours show the position of the singularities of the integrand in the θ, θ' plane. The arrows indicate the direction of increasing k/p .

where the function $g(k, p)$ is the result of the integration of Eq. (10) over \mathbf{p}' and \mathbf{k}' and the angular components of \mathbf{p} and \mathbf{k} . The leading term in $\delta\tau_T^{-1}$ is linear in temperature because of the jump $g(p+0, p) - g(p-0, p) = \Delta g(p)$ of the function g at $k = p$ resulting from the double pole at $(\theta, \theta') = (0, \pi)$ for $k = p$:

$$\delta\tau_T^{-1} = -\frac{n_{\text{def}}}{4\pi^4 v^2} \frac{\Delta g(k_F)}{v} T = -T \frac{2n_{\text{def}} k_F}{\pi \hbar^4 v^3} \Gamma_0 \tilde{V}(0), \quad (11)$$

$$\Gamma_0 = \int \frac{d\mathbf{n}}{2\pi} \text{Tr}[\hat{u} \hat{s}_{\mathbf{n}} \hat{u} \hat{s}_{-\mathbf{n}}] = \sum_{s,l=x,y,z} u_{sl}^2 (1 + \delta_{sz}).$$

When deriving $\Delta g(k_F)$ in Eq. (11), we took into account that the contribution to the jump of g comes from backscattering, $(\theta, \theta') = (0, \pi)$, so that we substituted $\mathbf{p} = \mathbf{k}$ and $\mathbf{p}' = -\mathbf{p}$ in all smooth angle-dependent functions. This produced the exchange term form factor $\Gamma_0 \equiv \langle \Gamma_{\mathbf{p}, -\mathbf{p}}^{\mathbf{p}, -\mathbf{p}} \rangle_{\mathbf{p}}$ averaged over the incidence angle and also resulted in the vanishing of the Hartree term due to the absence of backscattering of chiral electrons off the Coulomb potential $\tilde{\Gamma}_{\mathbf{p}, -\mathbf{p}}^{\mathbf{p}, -\mathbf{p}} = 0$.

Finally, we arrive at the following expression for the dominant temperature-dependent part of the resistivity:

$$R(T) - R(0) = -\frac{h}{e^2} \frac{4T\tilde{V}(0)}{\hbar v^2 \epsilon_F \tau_*}, \quad \tau_*^{-1} = \frac{\pi \gamma n_{\text{def}}}{\hbar} \Gamma_0. \quad (12)$$

It is interesting to compare the latter result with that derived [3] for electrons in a simple-band 2D semiconductor or metal. In the latter case, $R(T)$ is formed by the competition of the Hartree and Fock contributions which have different signs, which may lead to the change of the size and even the sign of the effect upon variation of the electron density or spin polarization of the 2D gas by an external magnetic field. In graphene, the T -dependent correction to the resistivity is only due to the exchange interaction, so that it is negative and its density dependence tracks the density dependence of the interaction constant $\tilde{V}(0)$. For a 2D-screened Coulomb interaction $\tilde{V}(q) = 2\pi(e^2/\chi)/(q + \kappa)$, we estimate $\tilde{V}(0) = \frac{1}{4}\gamma^{-1}$, which leads to the result in Eq. (1). The other difference between graphene and usual semiconductor structures is that in the former the linear in T correction is caused only by atomically sharp disorder (e.g., structural defects in graphene, chemical deposits, substitutional disorder, and contact with an incommensurate lattice of a substrate), whereas in the latter it is formed by all scatterers. This means that the temperature dependence of resistivity should be weak (or even absent) in a suspended graphene sheet or a sheet loosely attached to the substrate and that it can be pronounced in devices where graphene is strongly coupled to the substrate.

In conclusion, we described the Friedel oscillations induced by scatterers in graphene and their effect on the resistivity. The general form of FO is given in Eq. (8). One of the immediate implications of this result is a r^{-2} dependence of the RKKY interaction between two magnetic

impurities in graphene. This is because a substitution atom with spin \mathbf{S} will generally create a perturbation $(\mathbf{S} \cdot \mathbf{s}_e)\hat{u}$ for the electron spin \mathbf{s}_e with \hat{u} containing all symmetry-breaking terms in Eq. (3). We also showed that, due to the chirality of graphene electrons, the linear temperature correction to the resistivity [Eqs. (1) and (12)] is caused by atomically sharp defects rather than by Coulomb charges in the insulating substrate, so that its measurement can be used as a tool to test the microscopic composition of disorder.

We thank I. Aleiner and A. Ludwig for discussions. This project was funded by EPSRC Grant No. EP/C511743.

-
- [1] J. Friedel, *Philos. Mag.* **43**, 153 (1952).
 - [2] K. H. Lau and W. Kohn, *Surf. Sci.* **75**, 69 (1978).
 - [3] G. Zala, B. N. Narozhny, and I. L. Aleiner, *Phys. Rev. B* **64**, 214204 (2001); **64**, 201201 (2001); **65**, 020201 (2002).
 - [4] S. Das Sarma and E. H. Hwang, *Phys. Rev. Lett.* **83**, 164 (1999); *Phys. Rev. B* **69**, 195305 (2004).
 - [5] A. M. Rudin, I. L. Aleiner, and L. I. Glazman, *Phys. Rev. B* **55**, 9322 (1997).
 - [6] F. Stern, *Phys. Rev. Lett.* **44**, 1469 (1980); A. Gold and V. T. Dolgoplov, *Phys. Rev. B* **33**, 1076 (1986).
 - [7] Y. Y. Proskuryakov *et al.*, *Phys. Rev. Lett.* **89**, 076406 (2002); Z. D. Kvon *et al.*, *Phys. Rev. B* **65**, 161304(R) (2002); A. A. Shashkin *et al.*, *Phys. Rev. B* **66**, 073303 (2002); V. M. Pudalov *et al.*, *Phys. Rev. Lett.* **91**, 126403 (2003); S. A. Vitkalov *et al.*, *Phys. Rev. B* **67**, 113310 (2003).
 - [8] K. S. Novoselov *et al.*, *Science* **306**, 666 (2004); K. S. Novoselov *et al.*, *Nature (London)* **438**, 197 (2005).
 - [9] Y. Zhang *et al.*, *Nature (London)* **438**, 201 (2005); *Phys. Rev. Lett.* **94**, 176803 (2005).
 - [10] R. Saito, G. Dresselhaus, and M. S. Dresselhaus, *Physical Properties of Carbon Nanotubes* (Imperial College Press, London, 1998).
 - [11] K. Nomura and A. H. MacDonald, *Phys. Rev. Lett.* **96**, 256602 (2006); T. Ando, *J. Phys. Soc. Jpn.* **75**, 074716 (2006).
 - [12] E. McCann *et al.*, *Phys. Rev. Lett.* **97**, 146805 (2006).
 - [13] I. L. Aleiner and K. B. Efetov, cond-mat/0607200.
 - [14] Corners of the hexagonal Brillouin zone are $\mathbf{K}_{\xi} = \xi(\frac{4}{3}\pi a^{-1}, 0)$, where $\xi = \pm 1$ and a is the lattice constant. In the basis $[\phi_{\mathbf{K}_{+,A}}, \phi_{\mathbf{K}_{+,B}}, \phi_{\mathbf{K}_{-,B}}, \phi_{\mathbf{K}_{-,A}}]$, time reversal $T(W)$ of an operator W is described by $T(\hat{W}) = (\Pi_x \otimes \sigma_x) W^* (\Pi_x \otimes \sigma_x)$. This can be used to show that $T(\Sigma_s) = -\Sigma_s$, $T(\Lambda_l) = -\Lambda_l$, and $T(\Sigma_s \Lambda_l) = \Sigma_s \Lambda_l$.
 - [15] E. Fradkin, *Phys. Rev. B* **33**, 3257 (1986); E. McCann and V. Fal'ko, *Phys. Rev. B* **71**, 085415 (2005); M. Foster and A. Ludwig, *Phys. Rev. B* **73**, 155104 (2006).
 - [16] S. V. Morozov *et al.*, *Phys. Rev. Lett.* **97**, 016801 (2006).
 - [17] T. Ando, T. Nakanishi, and R. Saito, *J. Phys. Soc. Jpn.* **67**, 2857 (1998).
 - [18] V. Cheianov and V. I. Fal'ko, *Phys. Rev. B* **74**, 041403(R) (2006).
 - [19] The $1/r^2$ FO in a gas of relativistic 2D fermions vanish in the massless limit. See D. H. Lin, *Phys. Rev. A* **73**, 044701 (2006).